

Direct Recovery of the Camera Internal Parameters Using Known Angles

Marina Kolesnik

Fraunhofer Institute for Media Communication, Schloss Birlinghoven, D-53754 Sankt Augustin, Germany.
marina.kolesnik@imk.fraunhofer.de

Abstract

We address the problem of direct internal calibration of a camera from a set of known angles between optical rays. A pen-size laser crosshair projector is used to generate a reference pattern whose angular features are known. Each known angle between a pair of optical rays imposes one angular constraint on the internal camera parameters. Several constraints form a system of equations, which is solved for the internal parameters. Because the angular constraints are given in the standard coordinate system of the camera, the internal parameters are recovered directly, that is without referring to any world coordinate system. An advantage that follows, is that calibration does not require precise measurements of 3-D coordinates of reference points. The final calibration parameters as well as the first order radial distortion parameter are computed by nonlinear optimization. We analyze an accuracy of angular values between optical rays and present experimental results of camera calibration. Angular calibration is fast, robust and easy to implement method, which is suitable for quick "off-lab" calibration of cameras.

1. Introduction

Recent advances in camera self-calibration could not yet eliminate standard calibration from those computer vision applications where metric information is essential. Numerous articles on the subject of camera calibration, which have been published recently, confirm continuous interest in the problem. Below we review only some recent publications out of the enormously large field of research dedicated to camera calibration and self-calibration.

Vast majority of photogrammetric calibration techniques uses precise distance measurements for a set of 3-D reference points. The classical Direct Linear Transform (DLT) calibration method [1], [22] recovers the 5 internal and 6 pose parameters of a fully projective camera from the images of at least 6 known 3D points by solving a system of linear equations. The disadvantage of the DLT is that it deals with the ideal projective camera model, which means that optical distortion has to be removed beforehand. Also, the entries of the camera perspective projection matrix recovered by the DLT depend on some irrelevant coordinate system where the

actual reference measurements were done. Finally, the perspective projection matrix ought to be broken down into the internal and the pose parameters of the camera [7]. Despite of cumbersome implementation, the DLT is widely popular in the computer vision community [30], [6]. A calibration technique that became classical was proposed by Tsai in [29] and developed further in [13]. It recovers the intrinsic and optical distortion parameters from the nonlinear equations describing the projection of 3-D points onto pixels. A complete set of the camera internal parameters and the first order radial distortion parameter is computed as a result of nonlinear optimization.

Recently developed DLT-like methods consider a more restrictive camera model by assuming that some internal parameters (these are normally aspect ratio and skew) are pre-calibrated [8], [21], [5], [28]. For example the "4-points" method suggested by Triggs in [28] assumes that the focal length is the only unknown internal parameter, whereas the "5-points" one considers both the focal length and the principal point as unknowns. However the performance analysis made Triggs indicates that traditional "6-points" DLT calibration is always preferable compared to the 4- and 5-points methods when there are more than six 3-D reference points available.

Contrary to DLT-like calibration, self-calibration does not use any calibration object [16], [20]. The rigidity of the scene provides in general two constraints on the internal parameters of the moving camera from its single displacement. Consequently, correspondences between three images taken by the same camera with fixed internal parameters are sufficient to recover both the internal and the pose parameters [15], [9]. It was shown that self-calibration can be applied for a camera with varying focal length and principal point, but fixed aspect ratio and zero skew [5], [11], [18]. However, the problem that was not addressed is the varying lens distortion for a zooming camera: changes in distortion parameters are noticeable and applying the pinhole model to undistorted images can not be justified. While self-calibration approach is flexible, it is not stable [2]: the results are not always reliable because there are many parameters to estimate. In addition, there are several types of camera motion, for which self-calibration is a degenerate problem, i.e. there exist ambiguous solutions [24]. Serious numerical instabilities occur for one of the most natural imaging situation when the camera moves on a sphere and focuses

the sphere’s center: the focal length can not be estimated even when the other intrinsic parameters are known [26].

Since traditional calibration uses known world coordinates, and advanced self-calibration is generally not stable, neither is suitable for quick “off-lab” calibration of cameras. Other calibration techniques tried to tackle the problem by using vanishing points for orthogonal directions [3], [14], geometric objects like spheres [17] or planar surfaces [25], [27], [31], whose images display invariant properties, or special camera motion [4], [10], [23].

A fact exploited by angular calibration is that a projective camera is uniquely defined by a certain number of optical rays. In our calibration setup a laser crosshair generates a specific geometrical pattern. The image of the crosshair footprint contains a set of pixel pairs whose angular configuration is known. Each pair of pixels defines a non-linear constraint on the internal camera parameters. When several constraints are put together, a system of equations is formed. This system is solved for the camera internal parameters.

The work of Stein [23] is the most closely related with this paper and we would like to point out the differences. Stein’s calibration method also exploits angles but uses them in the “reverse” order. A highly accurate rotary platform provides pure rotations of the camera. This requires special mechanical equipment. The angles of rotations are measured and used in the minimization process to make them consistent with the camera internal parameters.

The paper is organized in 4 Sections. In Section 2.1 an experimental setup for angular calibration is described. The mathematical model used for angular calibration is given in Section 2.2. Maximum likelihood solution for the projective camera model is described in Section 2.3. Section 2.4 deals with optical distortion. Accuracy of the angular values is investigated in Section 2.5. Experimental results of calibration are given in Section 3. Concluding remarks are made in the last section.

2. Angular Calibration

2.1 The calibration setup

An experimental setup for calibration includes a camera and a pen-size laser crosshair projector. ([12], Figure 1, left) The laser is equipped with an optical head, which splits its beam into two planar sheets. When these are projected onto a plane, the laser footprint is a cross. A fan angle of the laser, subtended by the point of crosshair origin (i.e. the point where the two planar sheets originate) and the end points of the projected crosshair footprint, is known with high accuracy.

In the calibration setup, both the camera and the laser are attached next to each other and are fixed on a tripod so

as to ensure the closest possible location of the camera optical center and the laser beam. In practice, we simply tape the camera and the laser together before fixing them on the tripod. The whole procedure takes about 5 minutes. One condition must hold: the viewing angle of the camera must exceed the fan angle of the laser crosshair, so that the camera observes the end points of the crosshair footprint in its field of view. If the above mentioned conditions are satisfied, the image of the footprint merely depends on the shape of objects the laser crosshair is projected upon. This is easy to see if we consider a thought experiment where 1) the camera optical center coincides with the crosshair origin and 2) the camera axis is parallel to the laser beam. In this case, it is quiet clear that the footprint image will not depend on the shape of scene objects at which the laser is projected. In reality, however, a small displacement between the camera and the laser origin can not be avoided. This causes slight variations in the shape of the footprint image.

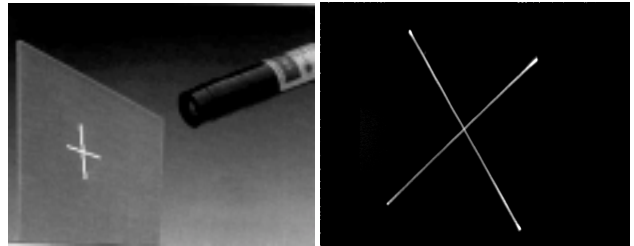


Figure 1. Left: Laser crosshair projector: commercial product of LASIRIS Inc. Right: Undistorted footprint image used for calibration.

However, if the distance between the crosshair origin and 3-D points highlighted by its footprint on a scene is much larger than the distance between the camera and the laser, the difference in angles that the projected footprint points subtend with respect to the camera optical center and the crosshair origin will be minuscule. We, therefore, assume that the angle between a pair of optical rays, defined by two pixels that are images of the two “opposite” endpoints on the footprint, is equal to the laser’s fan angle. In fact, we shall show that for any realistic calibration setup a relative error for this angle does not exceed 0.6%. The endpoints and the center of the crosshair footprint are clearly seen from large distances and can be accurately extracted in the image. All these make the angular calibration technically easy and reliable.

2.2. Angular relations

We consider a full projective pinhole camera model as in [7]. The 3×4 perspective projection matrix $\tilde{\mathbf{P}}$ depends on the five internal parameters. When $\tilde{\mathbf{P}}$ is expressed in the coordinate system attached to the camera (i.e. standard coordinate system with its origin in the optical center, axis

Z along the optical axis and the image plane defined by the axis X and axis Y) it is given by:

$$\tilde{\mathbf{P}} = \begin{bmatrix} -\alpha_u & \alpha_u \cot \theta & u_0 & 0 \\ 0 & -\alpha_v / \sin \theta & v_0 & 0 \\ 0 & 0 & 1 & 0 \end{bmatrix} \quad (1)$$

where α_u, α_v are the *scaling factors*, (u_0, v_0) is the *principal point* and θ is the camera's *skew angle*. Consequently, five constraints on the camera internal parameters, given in the standard coordinate system, define the camera model fully.

Consider a 3-D line $\langle C, m \rangle$ defined by a pixel m and the camera optical center C as in Figure 2. In the standard coordinate system this line, which is called the optical ray defined by m , is given by:

$$\mathbf{M} = \lambda \mathbf{P}^{-1} \tilde{\mathbf{m}} \quad (2)$$

where \mathbf{P} is the leftmost 3x3 submatrix of $\tilde{\mathbf{P}}$, and $\tilde{\mathbf{m}} = [m_1, m_2, 1]$ is the homogeneous coordinate vector of m . The end point of the 3-D vector \mathbf{M} gives a point M on the optical ray $\langle C, m \rangle$ as λ varies between $-\infty$ and $+\infty$.

Consider a pair of pixels m and n , which are the images of the "opposite" end points of the crosshair footprint M and N . Let $\langle C, m \rangle, \langle C, n \rangle$ be the two optical rays, defined by m and n , respectively. Each optical ray can be expressed in the form of equation (2). Now, take into account that distances from L and C to any of the footprint points in the object space such as S, N, M, Q and O , are at least ten times that of the distance between L and C . Under this assumption, the angle between the optical rays $\langle C, m \rangle$ and $\langle C, n \rangle$ is practically equal to the fan angle γ subtended by the rays $\langle LM \rangle$ and $\langle LN \rangle$. A scalar product of the two 3-D vectors which define $\langle C, m \rangle$ and $\langle C, n \rangle$ expresses this assumption:

$$\mathbf{M}^T \mathbf{N} = |\mathbf{M}| |\mathbf{N}| \cos \gamma \quad (3)$$

Here \mathbf{M} and \mathbf{N} be the two 3-D vectors that define $\langle C, m \rangle$ and $\langle C, n \rangle$, respectively. Expansion of (3) to pixel coordinates using (1) and (2) for the camera with zero skew ($\theta = 90^\circ$) yields:

$$\begin{aligned} & \frac{(u_0 - m_1)(u_0 - n_1)}{\alpha_u^2} + \frac{(v_0 - m_2)(v_0 - n_2)}{\alpha_v^2} + 1 = \\ & = \cos \gamma \sqrt{\frac{(u_0 - m_1)^2}{\alpha_u^2} + \frac{(v_0 - m_2)^2}{\alpha_v^2} + 1} \times \\ & \quad \times \sqrt{\frac{(u_0 - n_1)^2}{\alpha_u^2} + \frac{(v_0 - n_2)^2}{\alpha_v^2} + 1} \end{aligned} \quad (4)$$

Each laser crosshair footprint provides four independent constraints (angles) on the camera internal parameters. The two constraints are provided by the "opposite" endpoints of the footprint, whereas the other

two arise from a combination of the cross' center with the two endpoints which are not aligned. Therefore, given a single image of the crosshair, it is possible to calibrate a zero skew camera by solving a system of four equations such as (4).

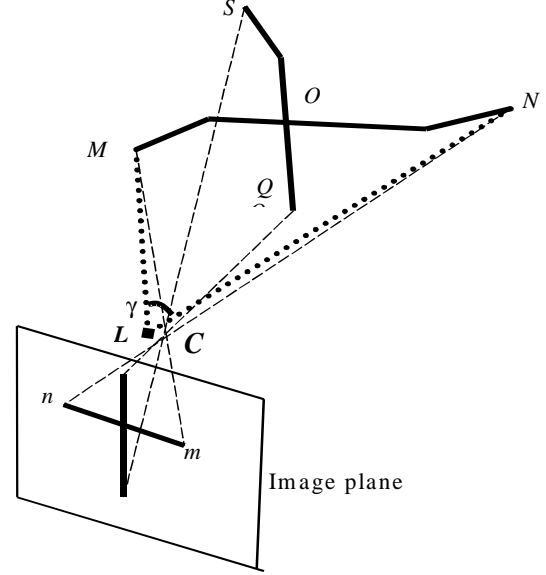


Figure 2. Geometry of the calibration setup. L is the crosshair origin, and C is the camera's optical center. Angle $\gamma = \angle MLN$ is the fan angle of the laser crosshair. $MSNQO$ is a 3-D footprint of the laser crosshair. Note, that four angles subtended by the footprint center O and each end point with respect to L , are half that of γ . $|LC|$ is a distance between L and C , which is small compared to a distance between L and any arbitrary point on the crosshair footprint.

Unfortunately there is no practical way to rewrite these equations in the form of a linear system for which the least squares technique is applicable. However, we have used equation (4) to estimate the initial values of the four internal parameters, which are then refined with nonlinear minimization. The procedure is as follows. Set the coordinates for the principal point to the coordinates of the central pixel of the image. Set α_u to the one of the image size. Pick up a pair of pixels that are the images of the opposite ends of the crosshair footprint and use their coordinates to set up equation (4) using also the values for α_u and (u_0, v_0) . This is a quadratic equation with respect to the variable $1/\alpha_v^2$. If the discriminant of this equation is positive, solve it for the positive real root and find the value for α_v . If the discriminant is negative, update the value for α_u so that it becomes positive and solve the quadratic equation once again to find estimation for α_v .

2.3. Maximum likelihood estimation

Final calibration for the full projective camera is obtained using more angular measurements. Let us assume

that we are given k images of laser crosshair footprints. Five reference points, namely end/center footprint points, are detected in each of the images. These points define four independent angular relations such as (4) for each image. Assuming that the image points are corrupted by independent and identically distributed noise, the maximum likelihood estimate for the parameters can be obtained with the least square approach. We minimize the sum of errors in the known angles over the whole set of the reference pairs of optical rays:

$$\sum_{i=1}^{4k} \left\| \frac{(\mathbf{M}_i^T \mathbf{N}_i)^2}{\|\mathbf{M}_i\|^2 \|\mathbf{N}_i\|^2} - \cos^2 \gamma_i \right\|^2 \quad (5)$$

where \mathbf{M}_i and \mathbf{N}_i are the 3D vectors which define the i -th pair of optical rays with the angle γ_i between them. γ_i is equal to the fan angle of the laser crosshair when the vectors \mathbf{M}_i and \mathbf{N}_i are subtended by the endpoints of the crosshair footprint, and it is equal to the half of the fan angle value if one of these vectors is subtended by the footprint's center. Combining (2) and (5) and introducing a symmetric matrix $\mathbf{B} = \mathbf{P}^{-T} \mathbf{P}^{-1}$, the target function (5) is given by:

$$\sum_{i=1}^{4k} \left\| \frac{(\tilde{\mathbf{m}}_i^T \mathbf{B} \tilde{\mathbf{n}}_i)^2}{(\tilde{\mathbf{m}}_i^T \mathbf{B} \tilde{\mathbf{m}}_i)(\tilde{\mathbf{n}}_i^T \mathbf{B} \tilde{\mathbf{n}}_i)} - \cos^2 \gamma_i \right\|^2 \quad (6)$$

Minimizing (6) by varying the values of the five parameters: $\alpha_u, \alpha_v, c, u_0, v_0$ is a nonlinear minimization problem, which is solved with the Levenberg-Marquardt algorithm as implemented in [19]. It requires an initial guess for the values of the unknown parameters, which is obtained as described at the end of the previous subsection.

2.4. Accounting for radial distortion

So far, we have assumed that pixel coordinates are not subjected to optical distortion. To account for lens aberration the undistorted coordinates (m_1, m_2) and (n_1, n_2) used in the angular relation (4) have to be substituted by their distorted counterparts (m_1^d, m_2^d) and (n_1^d, n_2^d) observed in the real image. To a good degree of accuracy lens aberration is modeled by radial distortion only and, moreover, for industrial machine vision applications only one term in approximation of radial distortion is needed. According to the broadly cited work of Tsai [29]: "any more elaborate modeling not only would not help but also would cause numerical instability". We, therefore, use the first order approximation for the ideal pixel coordinates in the image:

$$\begin{aligned} m_1 &= m_1^d + k_1(m_1^d - u_0)r^2 \\ m_2 &= m_2^d + k_1(m_2^d - v_0)r^2 \end{aligned} \quad (7)$$

where $r^2 = (m_1^d - u_0)^2 + (m_2^d - v_0)^2$. Combination of (7) and (6) defines the target function, which has to be minimized with respect to the complete set of the 5 internal parameters, i.e. $\alpha_u, \alpha_v, c, u_0, v_0$, and the radial distortion parameter k_1 . As before, this is solved with the Levenberg-Marquardt algorithm setting the initial value for k_1 to zero.

2.5. Accuracy of the angular values

Let us now investigate how accurate our assumption is concerning the angles between the end/center points of the crosshair footprint viewed by the camera. For simplicity, we consider the calibration setup in 2-D (Figure 3). As above, L is the crosshair origin and C is the camera optical center. The two 3-D points M and N are a pair of the "opposite" endpoints the projected footprint and γ is the fan angle of the laser. The distance d between the laser and the camera is much less than the distance from L to M or N , i.e. the ratios $d/d_s \ll 1$ and $d/d_t \ll 1$. Applying the cosine theorem to the triangles LMN and CMN , after some algebra we obtain:

$$\cos \gamma' = \frac{d^2 - d_s d \cos \varphi - d_t d \cos(\gamma + \varphi) + d_s d_t \cos \gamma}{\sqrt{d_s^2 + d^2 - 2d_s d \cos \varphi} \sqrt{d_t^2 + d^2 - 2d_t d \cos(\gamma + \varphi)}}$$

Using first order Taylor expansion in the small d we obtain the following approximation for the angle γ' :

$$\gamma' = \gamma + d \left(\frac{\sin(\gamma + \varphi)}{d_t} - \frac{\sin \varphi}{d_s} \right) \quad (7)$$

Assuming for instance that $d/d_s \sim d/d_t \sim 0.01$, and $\gamma \cong \varphi \cong 45^\circ$, the relative error for γ' is given by: $\delta\gamma/\gamma = 0.2\%$.

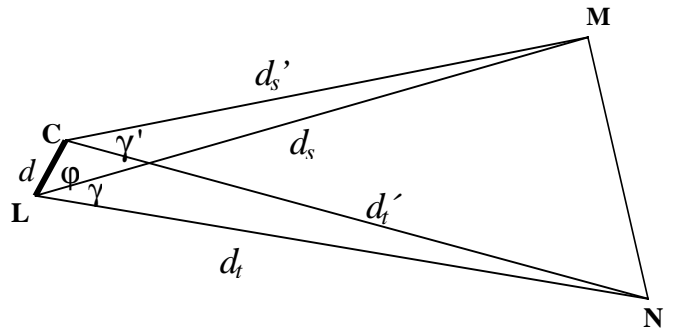


Figure 3. Geometry of the calibration setup in 2-D.

Similar geometrical consideration in 3-D suggests that:

$$\gamma' = \gamma + d \left(\frac{\sin(\gamma + \varphi)}{d_t} - \frac{\sin \varphi}{d_s} \right) + \frac{d}{d_s}$$

Consequently, the relative error for γ' in 3-D does not exceed 0.6%.

It follows from (7) that there is an optimal laser/camera setup when the difference between the angles γ' and γ is of second order in d :

$$\frac{\sin(\gamma + \varphi)}{d_t} = \frac{\sin\varphi}{d_s} \Rightarrow \varphi = \text{Arctg}\left(\frac{d_s \sin\gamma}{d_t - d_s \cos\gamma}\right) \quad (8)$$

Though it is difficult to provide the optimal value for the angle φ in practice, (8) still provides a certain rationale for the optimal adjustment of the calibration setup. Assuming, for instance, $d_s \approx d_t$ and $\gamma = 45^\circ$ the optimal value for the angle φ is about 80° .

3. Calibration results

The camera calibrated was the VS 500 CCD camera with 2.8 mm Iris lens (i.e. with $95^\circ/71^\circ$ horizontal / vertical angle of view). Image resolution was 640 x 486 pixels. The fan angle of the laser crosshair was equal to 60° . No special equipment except the camera and the laser projector fixed on the tripod was used for calibration. Four laser footprint images were acquired with the laser attached to the different sides of the camera, of which one example is shown in Figure 1, left. Neither care was taken concerning orientation of the laser crosshair or the shape of the surface the laser was projected at. Both the d/d_s and d/d_t distance ratio were at about 0.005. The initial values for the camera's skew and the distortion coefficient k_1 were set to zero. Final calibration was obtained by nonlinear optimization as described in Section 2.3.

It was observed that nonlinear minimization converges rapidly (for 3 iterations) on a stable minimum which remains the same even though initial values for the internal parameters vary by about 100% of their values. Both, the full projective model as well as the more restrictive model with zero skew were computed. One can see from Table 1, which lists the calibration results, that the camera has very small skew and noticeable non-square pixels.

Our calibration results were compared to the ones obtained by the DLT [6]. A rigid cubical frame of about 1m x 1m size with bright markers on the frame sides was used as a calibration target. The image was undistorted using the calibrated parameter k_1 . 3-D coordinates of the markers were precisely measured using photogrammetric technique. Pixel coordinates of the markers were localized accurately by a center of gravity algorithm. Two reference sets of 3-D and 2-D coordinates were the input to DLT calibration. The results of the DLT calibration given in the last column of Table 1 illustrate the convergence between the two calibration techniques.

	Angular ¹	Angular ²	DLT
α_u	331.59	330.75	322.73
α_v	419.12	420.37	415.17
α_u/α_v	1.26	1.27	1.28
u_0	295.02	294.62	282.1
v_0	234.13	236.02	234.03
θ	89.63°	90° -fixed	90° -fixed
k_1	-8.53e-7	-8.51e-7	None

Table 1. The internal calibration parameters computed by the angular and DLT calibration. First column: the results of angular calibration for the full projective model. Second column: the results of angular calibration assuming zero skew. Third column: the results of DLT calibration assuming zero skew.

4. Conclusions

We have presented a novel technique for direct internal calibration from known angles. A set of optical rays defined by the 3-D pattern as generated by the laser crosshair projector is computed. The angles between the pairs of optical rays from the set are known and used for calibration. The full projective camera model with the five internal parameters is considered. First, initial values of the four internal parameters are estimated. Second, the five internal parameters and the first order radial distortion parameter are computed with the maximum likelihood estimation. It takes about 3 iterations for nonlinear minimization to converge on a global minimum. Calibration appears to be pretty stable with regard to different initial values required by nonlinear minimization. The results of angular calibration are consistent with those ones obtained by the traditional DLT.

The novelty of angular calibration lies in the direct use of angles between the optical rays defined by particular points in the laser pattern (footprint ends, center). The method lies between DLT-like calibration and calibration from pure rotation, because it uses angular values –as in calibration from pure rotation - and these values form a reference set, instead of 3D reference coordinates used by the DLT calibration. The angular calibration is “one run” procedure that extends to many angles and finds an optimal solution by non-linear minimization of least squares.

Several advantages distinguish the angular calibration. First, it does not require any distance measurements, thus eliminating an extra source of errors. Second, angular calibration is specifically targeted on a direct recovery of the internal camera parameters while working naturally in the standard coordinate system. Third, the calibration setup is rather simple: all what is required is a small and low power consuming laser. Because the crosshair

generates a clear footprint image, it is easy to extract the center and endpoints which are critical for calibration.

The angular calibration does not challenge precise “in-lab” calibration techniques but rather suggests a quick alternative method for outdoor calibration. Given an initial guess for the internal parameters, the angular calibration can be converted into a fully automatic procedure. This, in turn, makes the idea attractive for the use by mobile robots. The technique is also directly applicable for calibration of cameras by images of stellar objects: the precisely known relationship between Earth and stellar objects that define angles between respective viewing rays may be used to set up the angular relations required for calibration.

References

- [1] Y. Abdel-Aziz and H. Karara. Direct linear transformation from comparator to object space coordinates in close-range photogrammetry. In *ASP Sym. Close-Range Photogrammetry*, pages 1-18, Urbana, Illinois, 1971.
- [2] S. Bougnoux. From projective to euclidean space under any practical situation, a criticism of self-calibration. In *Proceedings of ICCV'98*, pp.790-796.
- [3] B. Caprile and V. Torre. Using Vanishing Points for Camera Calibration. *Intern. J. of Computer Vision*. Vol. 4, 1990, pages 127-140.
- [4] F. Du and M. Brady. Self Calibration of the Intrinsic Parameters of Cameras for Active Vision Systems. In *Proc. of IEEE Conf. on Computer Vision and Pattern Recognition*. New York, NY, June 1993, pages 477-482.
- [5] R. Enciso, T. Viville and A. Zisserman. An affine solution to Euclidean calibration for a zoom lens. *ALCATECH'96*, Denmark, 21-26 July, 1996.
- [6] O.D. Faugeras and G. Toskani. The calibration problem for stereo. In *Proc. IEEE Conf. Computer Vision and Pattern Recognition*, pages 15-20, 1986.
- [7] O. Faugeras. Three-Dimensional Computer Vision. A Geometric Viewpoint. MIT Press, Cambridge, MA, pages 55-65, 1993.
- [8] R.M. Haralick, C. Lee, K. Ottenberg and M. Noelle. Analysis and solutions of the three point perspective pose estimation problem. In *IEEE Conf. Computer Vision and Pattern Recognition*, pages 592-598, 1991.
- [9] R. I. Hartley. An algorithm for self-calibration from several views. In *Proc. IEEE Conf. Computer Vision and Pattern Recognition*. Seattle, WA, June 1994, pages 908-912.
- [10] R. I. Hartley. Self-calibration from multiple views with a rotating camera. In *Proc. European Conf. Computer Vision*, pages 471-478, May, 1994.
- [11] A. Heyden and K. Aström. Euclidean Reconstruction from Image Sequences with Varying and Unknown Focal Length and Principal Point. In *IEEE Conf. Computer Vision and Pattern Recognition*, Puerto Rico, 1997.
- [12] Laser Crosshair Projector LAS-635-15. Commercial Product of LASIRIS Inc.
- [13] R.K. Lenz and R.Y. Tsai. Techniques for Calibration of the Scale Factor and Image Center for High Accuracy 3-D Machine Vision Metrology. *IEEE Trans. Pattern Anal. Machine Intell.* Vol.10, 1988, pages 713-720.
- [14] D. Liebowitz and A. Zisserman. Metric rectification for perspective images of planes. In *Int. Conf. Computer Vision and Pattern Recognition*, pages 382-488, 1998
- [15] Q.-T. Luong and O. Faugeras. Self-calibration of a moving camera from point correspondences and fundamental matrices. *The International Journal of Computer Vision*, 22(3):261-289, 1997.
- [16] S. J. Maybank and O. D. Faugeras. A Theory of Self-Calibration of a Moving Camera. *International Journal of Computer Vision*. 8:2, pages 123-151, 1992.
- [17] M.A. Penna. “Camera Calibration: A quick and Easy Way to Determine the Scale Factor”. *IEEE Trans. Pattern Anal. Machine Intell.* Vol.13, 1991, pages 1240-1245
- [18] M. Pollefeys, R. Koch and L.V. Gool. Self-Calibration and Metric Reconstruction in spite of Varying and Unknown Internal Camera Parameters. *Proc. of Inter. Conf. on Computer Vision*. pages 90-95, 1998.
- [19] W.H. Press, S.A. Teukolsky, W.T. Vetterling and B.P. Flannery. Numerical Recipes in C. Cambridge University Press, pages 683-688, 1996.
- [20] L. Quan. Self-Calibration of an Affine Camera from Multiple View. *International Journal of Computer Vision*. 19(1), pages 93-105, 1996.
- [21] L. Quan and Z.D. Lan. Linear $n \geq 4$ -point pose determination. In *IEEE Int. Conf. Computer Vision*, 1998.
- [22] C.C. Slama, ed. *Manual of Photogrammetry*. 4th edition. American Society of Photogrammetry, 1980.
- [23] G. P. Stein. Accurate Internal Camera Calibration using Rotation, with Analysis of Sources of Error”. In *Proc. of Inter. Conf. on Computer Vision*. 1995.
- [24] P. Sturm, Critical Motion sequences for Monocular Self-Calibration and Uncalibrated Euclidean Reconstruction. In *Proc. Conf. Computer Vision and Pattern Recognition*, pp. 1,100-1,105, June 1997.
- [25] P. Sturm and S. Maybank. On plane-based camera calibration: A general algorithm, singularities, applications. In *IEEE Conf Computer Vision and Pattern Recognition*, 1999.
- [26] P. Sturm. A Case Against Kruppa’s Equations for Camera Self-Calibration. *IEEE Transactions on Pattern Analysis and Machine Intelligence*. Vol.22, No. 10, October 2000.
- [27] B. Triggs. Autocalibration from planar surfaces. In *Proc. of European Conf. Computer Vision*, pages 89- 105, June 1998.
- [28] B. Triggs. Camera Pose and Calibration from 4 or 5 known Points. In *IEEE Int. Conf. Computer Vision*, pages 278- 284, September 1999.
- [29] R.Y. Tsai, “A Versatile Camera Calibration Technique for High-Accuracy 3D Machine Vision Metrology Using Off-the-Shelf TV Cameras and Lenses”. *Journal of Robotics and Automation*, Vol.3(4),1987, pages 323-344.
- [30] J. Weng, P. Cohen and M. Herniou. Camera Calibration with Distortion Models and Accuracy Evaluation. *IEEE Trans. Pattern Anal. Machine Intell.* Vol.14, 1992, pages 965-980.
- [31] Z. Zhang. Flexible Camera Calibration By Viewing a Plane From Unknown Orientations. In *Proc. IEEE Conf. Computer Vision*, pages 666-673, September 1999.